ChemPubSoc Europe

DOI: 10.1002/chem.201600581

CHEMISTRY
A European Journal
Full Paper

Fluorescent Probes

Rational Design of Push–Pull Fluorene Dyes: Synthesis and Structure–Photophysics Relationship

Janah Shaya, Fabien Fontaine-Vive, Benoît Y. Michel, and Alain Burger*[a]

Dedicated to the memory of Professor Guy Ourisson

Abstract: Our work surveyed experimental and theoretical investigations to construct highly emissive D–π–A (D = donor, A = acceptor) fluorenes. The synthetic routes were optimised to be concise and gram-scalable. The molecular design was first rationalised by varying the electron-withdrawing group from an aldehyde, ketotriazole or succinyl to methylenemalonitrile or benzothiadiazole. The electron-donating group was next varied from aliphatic or aromatic amines to saturated cyclic amines ranging from aziridine to azepane. Spectroscopic studies correlated with TD-DFT calculations provided the optimised structures. The selected push–pull dyes exhibited visible absorptions, significant brightness, important solvatofluorochromism, mega-Stokes shifts (> 250 nm) and dramatic shifts in emission to the near-infrared. The current library includes the comprehensive characterization of 16 prospective dyes for fluorescence applications. Among them, several fluorene derivatives bearing different conjugation anchors were tested for coupling and demonstrated to preserve the photophysical responses once further bound.

Introduction

New fluorescent tools are in great scientific and economic demand.[1] In particular, push–pull dyes have emerged as a captivating area that has stimulated intense research for indispensable applications.[2–4] This class of dyes consists of a π-scaffold functionalised with an electron-donating or an electron-withdrawing group (EDG or EWG), respectively abbreviated as donor (D) and acceptor (A). This D–π–A system undergoes a photo-induced intramolecular charge-transfer (ICT) state, forming a low-energy molecular orbital (MO). Visible light provides sufficient energy to excite the electrons within this new MO, making these compounds generally coloured.[5] The ICT also generates dipole moments that augment the sensitivity of these fluorophores in response to polarity.[6,7] Dapoxyl[8,9] and Prodan[10–13] families are considered to be the state of the art among the solvatochromic dyes (Figure 1).

The aromatic framework in these probes plays a key role. Fluorene is a rigid, planar organic moiety with extended π-electron delocalization despite the absence of traditional auxochromic heteroatoms.[14] This is advantageous for fluorene because endocyclic heteroatoms in other spacers prompt non-radiative deactivation of the excited states, thus decreasing the fluorescence quantum yields.[15–17] The lack of auxochromes also prevents the forbidden n–π transitions that facilitate photodegradation.[18–20] Recently, Klymchenko and Konishi published fluorene-based analogues of Prodan (example **PP1**, Figure 1).[21] The analogues exhibited remarkable improvement in spectroscopic properties. Fluorenes manifest desirable red-shifted absorption and emission, enhanced brightness, photostability,[22–23] low cytotoxicity[24–25] and appreciable two-photon absorption cross-sections, allowing cell imaging with reduced photodamage.[21a] These specificities have made fluorenes a family of interest in biomedical research[26–32] as well as a cornerstone for the effective sensing of ions,[33–35] aggregation,[36–38] nucleic acids,[39–42] proteins,[43–44] biomembranes[45] and explosives.[46,47] The use of fluorenes also extends to vari-

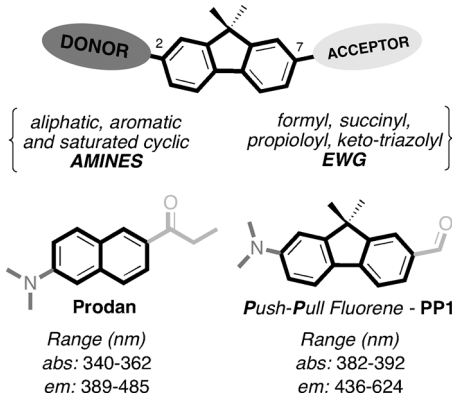

Figure 1. Structure of Prodan and the design of the D–π–A fluorenes in this study.

[a] J. Shaya, Dr. F. Fontaine-Vive, Dr. B. Y. Michel, Prof. Dr. A. Burger
Institut de Chimie de Nice, UMR 7272
Université de Nice Sophia Antipolis, CNRS, Parc Valrose
06108 Nice Cedex 2 (France)
E-mail: burger@unice.fr

Supporting information for this article and ORCIDs are available on the WWW under http://dx.doi.org/10.1002/chem.201600581.

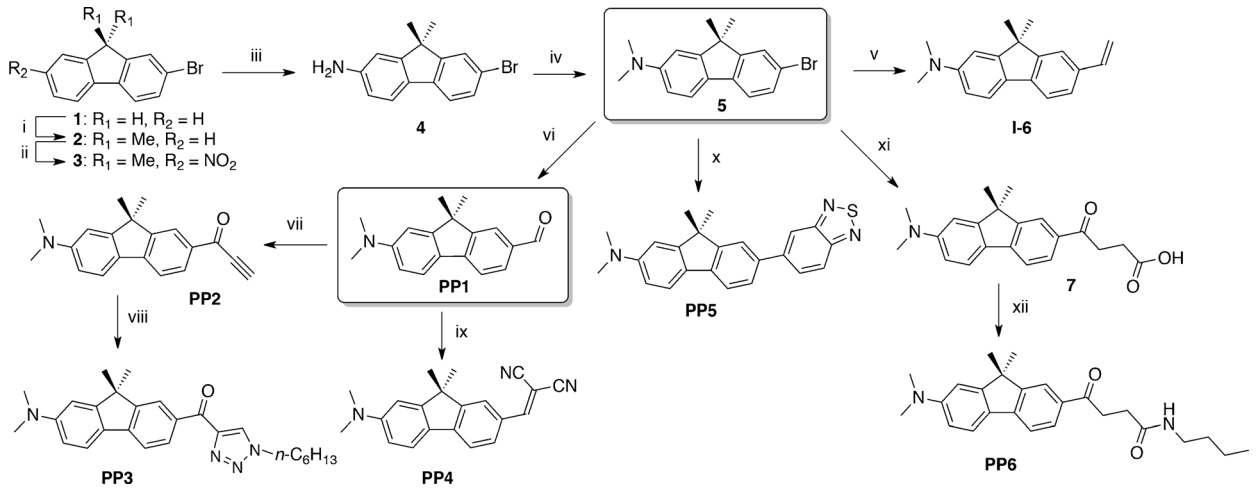

Scheme 1. Synthetic pathways leading to **PP1**–**6**. Reaction conditions: i) KOH (4 equiv), KI (0.1 equiv), MeI (2.3 equiv), DMSO, rt, overnight, 93%; ii) HNO_3, AcOH, rt, 2 h, 73%; iii) Fe (3 equiv), NH_4Cl (2 equiv), $EtOH_{(aq)}$, 80 °C, 4 h, 72%; iv) $(CH_2O)_n$ (5 equiv), $NaCNBH_3$ (3 equiv), AcOH, rt, overnight, 87%; v) $Pd(PPh_3)_4$ (5 mol%), tributylvinyltin (1 equiv), toluene, 80 °C, overnight, 80%; vi) *n*-BuLi (1.2 equiv), DMF (2 equiv), THF, −78 °C, 3 h, 70%; vii) (a) ethynylmagnesium bromide (1.4 equiv), THF, 0 °C, 2 h, (b) MnO_2 (15 equiv), DCE, 0 °C, 1 h, 98% (two steps); viii) *n*-hexN_3 (1.1 equiv), CuI (2 equiv), DIEA (5 equiv), AcOH (1 equiv), DCE, 3 h, 70%; ix) malonitrile (2 equiv), Al_2O_3 (4 equiv), toluene, overnight, 70 °C, 85%; x) (a) $Pd(PPh_3)_4$ (10 mol%), $Bu_3SnSnBu_3$ (1.3 equiv), toluene, 100 °C, 3 h, (b) $Pd(PPh_3)_4$ (10 mol%), 5-bromo-2,1,3-benzothiadiazole (2 equiv), 100 °C, overnight, 82%; xi) Mg (2 equiv), $BrCH_2CH_2Br$, succinic anhydride (2 equiv), THF, 60%; xii) DIC (1.1 equiv), HOBt (1.1 equiv), Et_3N (1.1 equiv), *n*-$BuNH_2$ (1.5 equiv), THF, rt, overnight, 72%.

ous optoelectronic devices[48–49] including solar cells,[50] laser diodes[51] and 3D data storage.[52,53]

In light of our work to find new fluorescent probes and practical applications,[54] we explored alternative synthesis to access to a library of 16 fluorene-based fluorophores adaptable for bioconjugation. Study and analysis of this family of fluorene derivatives have enabled the elucidation of the structure–photophysics relationship. Until now, few studies have attempted to elaborate such relationships in the field of chromophores.[55–57] This can be explained in the case of 2,7-disubstituted fluorenes, given that the reported syntheses involved diverse, demanding and lengthy multistep routes. Herein, we describe the straightforward microwave (MW)-assisted synthesis of fluorene push–pull dyes and the screening of the electron-withdrawing and donating abilities of the acceptor and the donor, respectively (Figure 1). Photophysical characterization combined with DFT calculations found the optimum D–π–A combination in terms of visible absorption, laser excitation accessibility, brightness and Stokes shift. Lastly, the strongest acceptor was engineered with two distinct donors to confirm the synergic effects of our rational design.

Abstract in French: Nous avons synthétisé des dérivés du fluorène comportant un groupe donneur (D) et accepteur (A) de type D–π–A très brillants et présentant différents points d'ancrage qui ne modifient pas la photophysique une fois conjugués. Leur conception rationnelle est basée sur une modification de la partie acceptrice A en criblant différents groupements électro-attracteurs tels que formyle, cétotriazolyle, succinyle, méthylènemalonitrile et benzothiadiazolyle. Quant à la partie donneuse, diverses amines aliphatiques, aromatiques et cycliques saturées de tension de cycle variée (de l'aziridine à l'azépane) furent introduites. Des études spectroscopiques combinées à des calculs TD-DFT ont permis d'identifier les fluorophores aux propriétés les plus remarquables. Les meilleures sondes absorbent dans le visible et démontrent une extrême brillance, un solvatofluorochromisme important et des déplacements de Stokes (>250 nm) conduisant à des émissions dans le proche IR. Cette librairie comprend ainsi 16 sondes prometteuses pour des applications en fluorescence.

Results and Discussion

Synthesis

First, various electron-withdrawing groups (EWG) with negative mesomeric or/and inductive effects were screened. Dimethylamine was chosen as the donor. With **PP1** and other fluorenes in the literature, as the formyl EWG is converted into an acetyl moiety, the absorption coefficient decreases and the maximum is blueshifted from the visible into the UV range.[21] These drawbacks limit the utility of such dyes. We aimed to introduce an EWG bearing an attachment point that retains the vital photophysical properties of the dye once bound as a biosensor. We envisaged the succinyl and propioloyl linkers as being compatible for peptide and click 1,3-dipolar couplings, respectively. Next, we incorporated benzothiadiazole and methylenemalonitrile, which are known to display prominent EW abilities.

The robust synthesis developed to access the fluorene derivatives **PP1**–**6** is outlined in Scheme 1. The synthesis was achieved by conventional methods,[21] namely C9-dimethylation, then regioselective mono-nitration followed by iron-mediated reduction to afford the amino intermediate **4** in 49% yield over three-steps. Reductive amination by using $NaCNBH_3$ and paraformaldehyde provided the key adduct **5** with the dime-

thylamino (D) group in 87% yield. Compound **5** was used to generate a variety of acceptors in addition to the interesting intermediate **I-6** bearing a vinyl group. The latter is a classical building block for fluorene materials prepared by metathesis[58] or Mizoroki–Heck cross-coupling;[59] yet, the effect of the vinyl group on the photophysics of our design has not been described. Primarily, halogen–metal exchange with *n*-BuLi on adduct **5** followed by treatment with DMF gave **PP1** in 70% yield. Grignard addition of the ethynyl group to **PP1** followed by oxidation by using MnO_2 at 0 °C generated the ethynyl ketone **PP2** in an excellent yield (98%). Noticeably, dimerization was observed when this reaction was allowed to proceed at room temperature for longer times. To test the effect of conjugation, **PP2** was converted into the ketotriazolyl derivative **PP3** in 70% yield with *n*-hexyl azide under copper-assisted azide–alkyne Huisgen cycloaddition (CuAAC). Next, the methylenemalonitrile was introduced by Knoevenagel condensation on the formyl of **PP1** in the presence of Al_2O_3 to yield **PP4** (85%).[60] Stille coupling of intermediate **5** and tributylvinyltin gave **I-6** in very good yield. The target **PP5** was obtained by coupling 5-bromo-2,1,3-benzothiadiazole to stannyl fluorene generated in situ. Lastly, the succinic linker was obtained by the formation of the Grignard of fluorene **5** at 60 °C and the subsequent addition of succinic anhydride in THF at 0 °C to give compound **7** in 60% yield. As a preliminary example of peptide functionalization, *n*-butyl amine was ligated to **7** using *N*,*N*′-diisopropylcarbodiimide (DIC) and l-hydroxybenzotriazole (HOBt) as activators to form **PP6** in 72% yield.

To evaluate the electron-donating groups (EDG), a concise two-step route was planned based on an efficient Pd-catalysed C–N cross-coupling protocol. The acceptor partner was always the carbaldehyde (Scheme 2). It is worth noting that, with the exception of some aromatic amines[28,61–64] and a few other donors,[47,65,66] incorporation of nitrogen nucleophiles into the fluorene scaffolds was not achieved easily. The previously described pathways involved long syntheses.[21,27,29] For instance, the introduction of aziridine was reported in five steps.[67] This encouraged us to examine a MW-assisted cross-coupling involving classically challenging amines such as azetidine and aziridine to determine the limits of the approach and to prepare the structurally-related fluorene dyes.

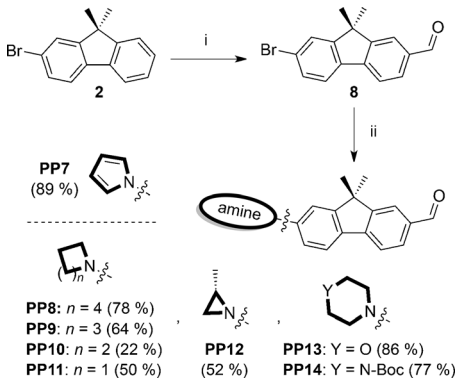

Scheme 2. Synthetic pathway leading to **PP7**–**14**. i) Cl_2CHOCH_3 (1.5 equiv), $ZrCl_4$ (1.5 equiv), CH_2Cl_2, 1 h, 0 °C, 77%; ii) amine (1.2 equiv), *t*BuONa (1.2 equiv), $Pd(OAc)_2$ (5 mol%), BINAP (10 mol%), toluene, MW (300 W/180 °C), 30 min.

Initially, formylation of fluorene at the C-7 position was optimised to obtain the key intermediate **8** suitable for amination (Scheme 2). Different formylating reagents, Lewis acids ($AlCl_3$, $TiCl_4$, $ZrCl_4$), solvents (THF, CH_3CN, CH_2Cl_2), temperatures and durations were assessed. Isolation of the different regioisomers proved to be a troublesome task. Nevertheless, the desired intermediate **8** was the exclusive product of the Friedel–Crafts reaction performed with $ZrCl_4$ and Cl_2CHOCH_3 in CH_2Cl_2 at 0 °C for 1 h. Subsequently, Buchwald–Hartwig amination of **8** was optimised by using different palladium catalytic systems with two activation sources (MW or thermal). Compounds **PP7**–**14** were thus synthesised by using $Pd(OAc)_2$, BINAP and NaO*t*Bu in toluene. MW radiation (300 W/180 °C) considerably reduced the reaction time from 12–30 h to 30 min and it was cleaner, with 5–10% enhanced yields in some cases (see the Supporting Information). Various cyclic aliphatic amines tolerated these reaction conditions and MW heating. The good to high coupling yields signify that the reductive elimination step was kinetically favoured over the β-hydride elimination in most catalytic cycles.[68] The defined route was rapid, efficient and gram-scalable.

Spectroscopic studies

Acceptor series

Unsymmetrical D–π–A fluorenes differing by their EWGs were characterised by UV and fluorescence in a wide range of solvents.[6] The photophysical properties in selected solvents are summarised in Table 1.

PP1,[21] with dimethylamino (D) and formyl (A) substituents, was set as the reference. The difference in wavelength ($\Delta\lambda = \lambda_{em} - \lambda_{abs}$) was employed to simplify the comparisons and as an indication of Stokes shift. Among the carbonyl acceptors, the triazolyl **PP3** absorbed as strongly as **PP1** ($38 \times 10^3\ M^{-1}cm^{-1}$ in dioxane), whereas **PP2** and **PP6** showed a two-fold hypochromicity (around $17 \times 10^3\ M^{-1}cm^{-1}$). The three carbonyl dyes absorbed in the visible range (370–413 nm in ethanol) and displayed particularly large Stokes shifts in polar solvents (e.g., 183–226 nm in ethanol). They showed gradually increased bathochromic shifts in their emission maxima when going from the most apolar aprotic solvent to the most polar solvent (Table 1, Figure 2). Compared to **PP1**, **PP3** presented a similar absorption, whereas the emission maximum was redshifted in polar solvents. By contrast, the absorption of **PP6** was blue-shifted, although the emission showed little changes (Figure 2 and Figure S1 in the Supporting Information). The quantum yields of **PP3** and **PP6** were in the range 52–86% in all of the tested solvents except in ethanol and water, where they were considerably reduced. Altogether, **PP3** demonstrated superior absorption and emission properties to those of **PP6**. Presenting benzothiadiazole (A), **PP5** revealed two distinct absorption maxima around 320 and 450 nm (Figure S1). This dye was only emissive in aprotic and non-polar solvents with mega-Stokes shifts (130–258 nm); a characteristic quite uncommon for solvatofluorochromic dyes in apolar media.[15] Among all the con-

Table 1. Spectroscopic properties of selected fluorophores with various EWG and the same dimethylamino donor.

Solvent $E_T(30)$[b]	λ, $\Delta\lambda$[c] [nm]	Fixed donor (NMe_2)/Varied acceptors[a]						
		PP1	**PP2**	**PP3**	**PP4**	**PP5**	**PP6**	**I-6**
				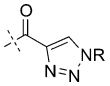		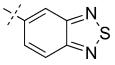	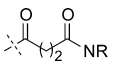	
ε [10^3 M^{-1} cm^{-1}][d]		35.5	17	38	33.5	27	16.5	30.5
H_2O (63.1)	λ_{abs}	386	421	nd[f]	501	446	373	353
	λ_{em}	624	615	nd	682	648	620	473
	$\Delta\lambda$	238	194	nd	181	202	247	120
	Φ[e]	0.04	0.005	nd	0.01	0.01	0.07	0.13
EtOH (51.9)	λ_{abs}	388	413	396	476	407	370	349
	λ_{em}	562	596	622	680	539	563	428
	$\Delta\lambda$	174	183	226	204	132	193	79
	Φ	0.48	0.11	0.06	0.12	0.01	0.71	0.5
CH_3CN (45.6)	λ_{abs}	384	409	389	474	404	368	350
	λ_{em}	521	620	578	679	498	523	432
	$\Delta\lambda$	137	211	189	205	94	155	82
	Φ	0.6	0.12	0.77	0.18	0.01	0.55	0.55
DMSO (45.1)	λ_{abs}	392	419	402	488	420	373	354
	λ_{em}	534	628	582	710	516	521	445
	$\Delta\lambda$	142	209	180	222	96	148	91
	Φ	0.9	0.18	0.85	0.19	0.02	0.72	0.75
$CHCl_3$ (39.1)	λ_{abs}	391	414	399	486	414	381	350
	λ_{em}	492	570	532	608	672	492	411
	$\Delta\lambda$	101	156	133	122	258	111	61
	Φ	0.62	0.34	0.72	0.45	0.04	0.54	0.02
dioxane (36)	λ_{abs}	382	405	391	467	409	364	350
	λ_{em}	453	509	488	583	593	456	395
	$\Delta\lambda$	71	104	97	116	184	92	45
	Φ	0.8	0.48	0.52	0.3	0.34	0.73	0.34
toluene (33.9)	λ_{abs}	387	407	394	474	413	374	346
	λ_{em}	436	490	473	566	548	450	388
	$\Delta\lambda$	49	83	79	92	135	76	42
	Φ	0.56	0.5	0.86	0.26	0.5	0.6	0.62

[a] Reported values are the average of two or more independent and reproducible measurements, ±1 nm for wavelengths. [b] Reichardt's parameter was employed to scale the polarity of the solvents.[6] [c] For convenience, Stokes shifts ($\Delta\lambda=\lambda_{em}-\lambda_{abs}$) are expressed in nm rather than in cm^{-1}. [d] Molar extinction coefficients (ε) in dioxane, relative standard deviations are equal to or less than 5%. [e] Quantum yields (Φ) were determined by using quinine sulfate in 0.1 M HCl solution ($\lambda_{ex}=350$ nm, $\Phi=0.54$)[69] or 4′-(dimethylamino)-3-hydroxyflavone in ethanol ($\Phi=0.27$)[70] as references, relative standard deviations are equal to or less than 15%. [f] Not determined, the compound was insufficiently soluble in water.

sidered acceptors, the methylenemalonitrile moiety **PP4** presented the most accentuated EW abilities, which translated into the largest redshift of both maxima (Figure 2).[71] The absorption was located in the blue spectral window (467–501 nm, Table 1), perfectly matching excitations with the argon laser line. The full width at half-maximum height of **PP4** is relatively narrow ($\Delta\lambda_{1/2}\approx 64$ and 82 nm, respectively), illustrating a useful asset for selective excitation (Figure 2). The intermediate **I-6** was emissive even in water (13%). Its fluorescence was quenched only in chloroform or upon adding 1% (v/v) of trifluoroacetic acid to 1,2-dichloroethane. The weak EW nature of the vinyl group accounts for the observed blueshifted absorption and emission. (Table 1, Figure S1). Reichardt's $E_T(30)$ scale was used to evaluate the sensitivity of the dyes to polarity, which followed the order: **PP4** > **PP3** > **PP1** ≈ **PP6** (slope comparison in Figure 3). The emission maximum was proportionally redshifted along the range of polarity. This quantitative parameter largely accounts for the dielectric constant of the solvent and its hydrogen-bond donor ability.[6] The strong positive solvatochromism in the dye emissions emphasises the large ICT character of their excited states. The latter was further substantiated by using the Lippert–Mataga model[72] (see the Supporting Information). The Stokes shifts were plotted as a function of the orientation polarizability in aprotic solvents as this model only takes into account the dipole–dipole interactions.

The plots demonstrate linear relationships and enable the estimation of the difference between the dipole moments of the ground and excited states ($\mu_E-\mu_G$, Figure S7 in the Supporting Information). The values of $\mu_E-\mu_G$ of 12.9, 13.5, 12.6 and 14.1 D were obtained for **PP1**, **PP3**, **PP6** and **PP4**, respectively. These results confirm the increase in the dipole moments in the excited states (Table S5 in the Supporting Information).

PP1, **PP4** and **PP6** were then investigated as representative examples in acetonitrile, chloroform and toluene by using DFT and time-dependant (TD)-DFT calculations. The DFT optimisation essentially gave geometries that were close to planar (Figure 4 and Scheme S4 in the Supporting Information). Simulations satisfactorily reproduced the entire absorption spectra with slight redshifts compared with the experimental values.

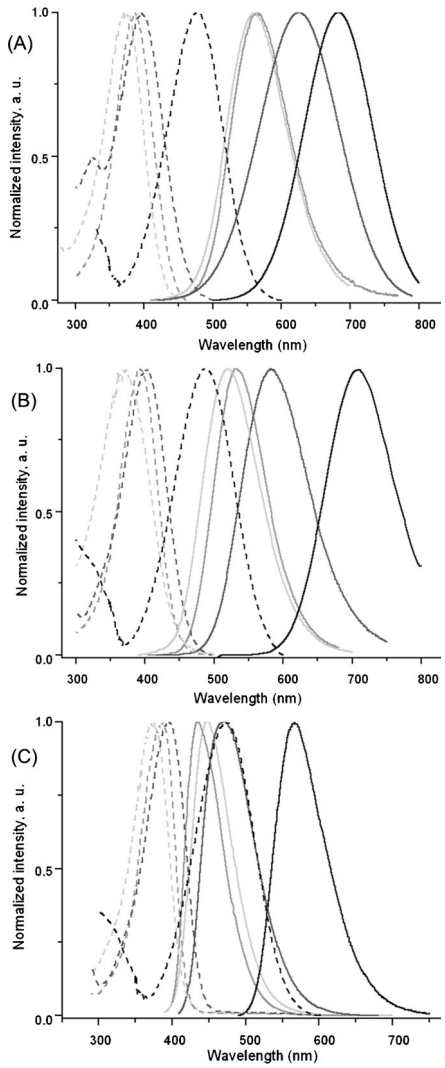

Figure 2. Absorbance (dashed lines) and emission (solid lines) spectra of **PP1** (mid grey), **PP3** (dark grey), **PP4** (black), **PP6** (light grey) in EtOH (A), DMSO (B) and toluene (C) as representatives of protic, aprotic polar and aprotic apolar solvents, respectively.

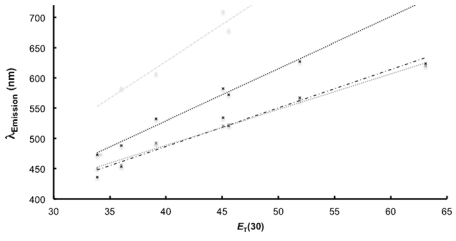

Figure 3. Dependence of the emission on the empirical polarity parameter $E_T(30)$ for selected acceptor-varied fluorenes **PP1** (black dash-dotted), **PP3** (black dotted), **PP6** (dark grey) and **PP4** (light grey). Correlation factors R^2 are, respectively, 0.97, 0.98, 0.99 and 0.93. The linear plots shown were obtained with all the tested solvents except for **PP4**, for which deviation from linearity was observed when protic solvents were included.

Calculations showed that the electronic transitions arose from electron promotion between the highest occupied molecular orbital (HOMO) and the lowest unoccupied molecular orbital (LUMO). In the frontier molecular orbitals, the HOMOs were localised at the fluorene and partially on the donor and the LUMOs at the acceptor and the benzene ring attached to it. Thus, the main contribution to the transition (ICT) dipole is in the plane of the molecule along the D–A axis (Figure 4, Scheme S4).

To sum up, these fluorophores exhibited important λ-shifts to the red in both their absorptions and emissions relative to Prodan. The absorption of the dyes was negligibly affected by polarity (<10 nm) except for the moderate bathochromic shift of **PP4** (35 nm). By contrast, all the considered dyes showed strong variations in their colours of emission. Hence, the prominent positive solvatofluorochromism confirms the presence of a strong ICT character only in the excited state. The modelling and calculations also support this conclusion. By contrast to the peptide-coupled product **PP6**, the conservation of the desired optical properties for **PP3** upon conjugation by CuAAC makes the ynone **PP2** a more attractive anchoring point for biolabelling (Table 1, Figure S1). The distinct photophysical behaviour of **PP5** makes it a prospective candidate for sensing hydrophobic environments such as lipid membranes by using a selective blue diode excitation.

Varied amine series

Different cyclic amines were characterised by using the carbaldehyde as a fixed acceptor. The main data are listed in Table 2.

PP7 (Table S4 in the Supporting Information) was established as the negative control given its blueshifted absorption and emission and its extremely low quantum yield ($<1\%$). Such characteristics were expected owing to the weak electron donation of the nitrogen's lone pair as part of the aromatic sextet of pyrrole. The DFT-calculated twisted geometry of the pyrrole and fluorene rings could also contribute to this poor donating ability (Figure S8 in the Supporting Information). Compared with **PP1**, the absorptions of the 4- to 7-membered amine rings of **PP8** and **PP10** were bathochromically shifted (10–15 nm, and 20–25 nm in water). The substitution of the methyl group by a longer alkyl chain redshifted the absorption maxima, in agreement with an increased inductive effect. By contrast, the 4- and 6-membered amine rings of **PP9** and **PP11** resulted in an unexpected hypsochromic shift (5–15 nm). Compounds **PP8**–**11** were strongly emissive except in water and gave almost similar fluorescence spectra along the solvent polarity (Table 2, Figure 5 and Figure S2 in the Supporting Information). Figure 6 depicts the dramatic Stokes shift and solvatofluorochromism of **PP9** as an example of this series.

Low quantum yields in water for solvatochromic dyes exhibiting strong ICT character are common. Introduction of the azetidine donor was reported to improve the quantum yield of sensors in aqueous media.[73–74] It was proposed that azetidine disfavours the formation of the poorly emissive, twisted internal charge-transfer (TICT) states in water. Applying this strategy to fluorene **PP11** was ineffective. The possibility of the formation of H-aggregates can be eliminated because the absorption maxima of the fluorene derivatives were not blueshifted in H_2O compared with other solvents.[75] Water molecules

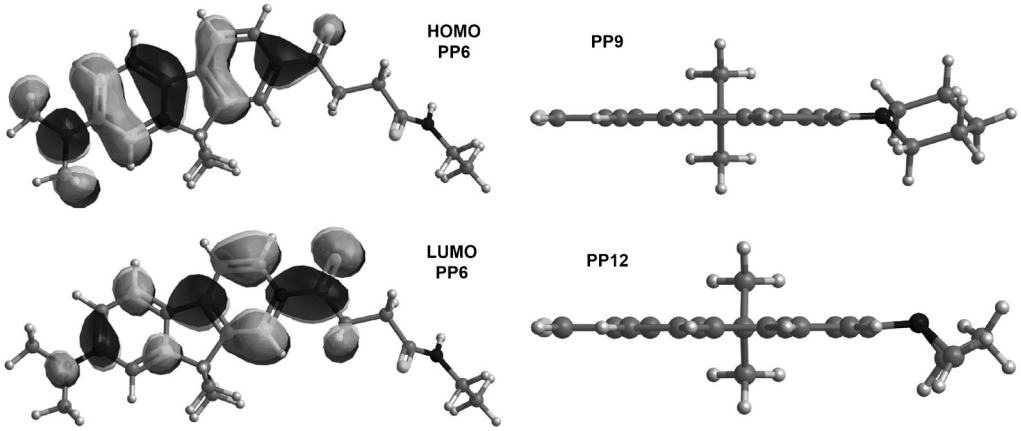

Figure 4. DFT and TD-DFT simulations. Ground-state optimised structures of **PP6**, **PP9** and **PP12**. Representation of the HOMO and LUMO frontier molecular orbitals of **PP6** (left). The peptide side chain in **PP6** was shortened to two carbon atoms to reduce the calculation time. Ground-state optimised structures of the coplanar **PP9** and bent **PP12** (right).

acting as an electron-trap for the excited species can possibly explain this result.[77] **PP12** was noticeably emissive contrary to the reported aziridine derivatives of other families like rhodamine.[73]

Compared with the other members of the series, this compound was characterised by reduced quantum yields in non-polar solvents and considerable hypsochromic shifts in the absorption and emission (Table 2 and Figure S2). It was proposed that the electron-donating ability of this three-membered het-

Table 2. Spectroscopic properties of selected fluorophores with various amines and the same formyl acceptor.

Solvent $E_T(30)$[a]	λ, $\Delta\lambda$[a] [nm]	Varied amines/Fixed acceptor (-CHO)[a]						
		PP8 	**PP9** 	**PP10** 	**PP11** 	**PP12** 	**PP13** 	**PP14** 
ε [10^3 M^{-1} cm^{-1}][a]		31.5	27.5	25	36	24	25	33
H_2O (63.1)	λ_{abs}	411	376	407	377	345	353	377
	λ_{em}	630	630	622	621	555	614	606
	$\Delta\lambda$	219	254	215	244	210	261	229
	Φ[a]	0.02	0.02	0.03	0.05	0.16	0.05	0.03
EtOH (51.9)	λ_{abs}	398	373	395	380	342	365	362
	λ_{em}	572	565	570	572	522	566	561
	$\Delta\lambda$	174	192	175	192	180	201	199
	Φ	0.45	0.38	0.45	0.44	0.33	0.41	0.44
CH_3CN (45.6)	λ_{abs}	397	376	391	377	351	365	362
	λ_{em}	528	530	532	532	483	518	518
	$\Delta\lambda$	131	154	141	155	132	153	156
	Φ	0.52	0.64	0.54	0.61	0.49	0.61	0.6
DMSO (45.1)	λ_{abs}	405	385	400	386	355	375	375
	λ_{em}	532	540	538	538	486	530	527
	$\Delta\lambda$	127	155	138	152	131	155	152
	Φ	0.84	0.93	0.77	0.84	0.64	0.78	0.84
$CHCl_3$ (39.1)	λ_{abs}	402	380	396	384	352	368	366
	λ_{em}	500	505	501	500	460	485	484
	$\Delta\lambda$	98	125	105	116	108	117	118
	Φ	0.62	0.65	0.62	0.48	0.46	0.68	0.58
dioxane (36)	λ_{abs}	394	375	391	375	350	365	363
	λ_{em}	454	456	454	462	450	450	449
	$\Delta\lambda$	60	81	63	87	100	85	86
	Φ	0.71	0.87	0.6	0.66	0.11	0.65	0.62
toluene (33.9)	λ_{abs}	397	371	394	378	352	365	365
	λ_{em}	440	447	439	442	428	429	449
	$\Delta\lambda$	43	76	45	64	76	64	84
	Φ	0.6	0.64	0.68	0.7	0.07	0.46	0.65

[a] As in Table 1.

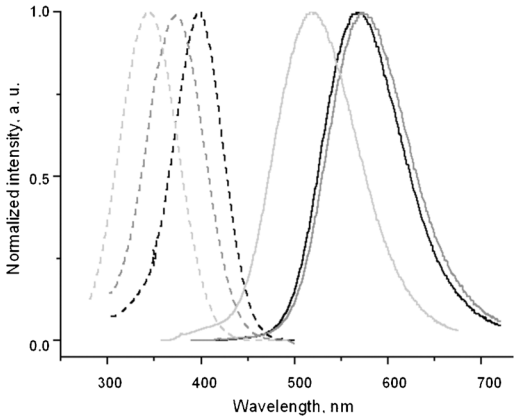

Figure 5. Absorbance (dashed lines) and emission (solid lines) of **PP8** (black), **PP9** (dark grey) and **PP12** (light grey) in EtOH.

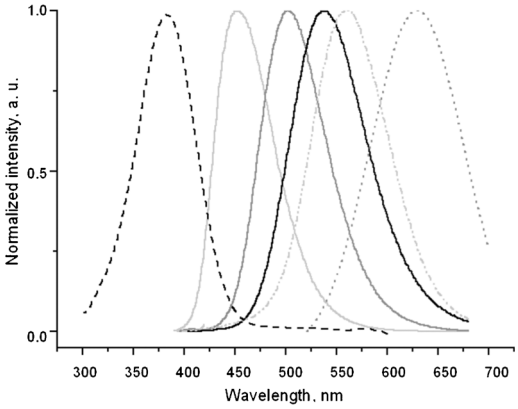

Figure 6. Absorbance (dashed line) and emission spectra of **PP9** in toluene (solid light grey), chloroform (solid dark grey), DMSO (black), EtOH (dash-dotted light grey) and H_2O (dotted dark grey). As the absorption is weakly solvatochromic, one representative spectrum is depicted.

erocycle was diminished[77] owing to the increased s character of the orbital of nitrogen atom's lone pair and the structurally and electronically enforced pyramidalised nitrogen.[78] This proposal was ascertained with the bent DFT structure of **PP12** compared with the coplanar fluorene–piperidine **PP9** (Figure 4). The sum of the three C-N-C bond angles (304° versus 333° for trimethylamine) confirms the pyramidalised geometry of the aziridine nitrogen and the planar geometry (348° versus 360° for trigonal geometry) of the piperidine nitrogen. Control analysis of aziridine versus the 2-methylaziridine derivative proves that the added methyl has no effect on the geometric parameters (Scheme S4).[79] The $\mu_E-\mu_G$ value of **PP12**, determined by the Lippert–Mataga model, was the lowest in this series (11.4–13.7 D, Table S4 and Figures S6–S7), thus attesting to its weaker donating ability.

Regarding the series of cyclic amines, **PP8**–**11** showed perfect overlap of the emission dependence on $E_T(30)$, implying a marginal effect of the ring size (between 4- and 7-membered rings) on the fluorescence properties (Figure S3). Interestingly, the strong quenching in water and significant brightness of these dyes in environments of distinct polarities opens opportunities to develop turn-on sensors upon shielding from water.[54] Aziridine (**PP12**) appeared as the weakest donor among all the considered aliphatic amines. As this functional group is well-known for cycloadditions in the area of fullerene–fluorophore organic devices,[63,68,79,80] a straightforward synthesis to **PP12** is highly in demand. Hence, such a conjugation should convert this dye into a 5-membered ring adduct easily detected by a typical redshift.

The presence of another heteroatom in the D group was studied with morpholine **PP13** and its piperazinyl analogue **PP14**, comprising a second amine for subsequent peptide coupling. Compared with **PP9**, which has a similar 6-membered amine ring, the introduction of nitrogen or oxygen blueshifted the absorption maxima, indicating that the negative inductive effect of the second heteroatom had imposed charge redistribution (Table 2 and Figure S4). The emissions of **PP13**–**14** showed bathochromic shifts with little deviations relative to the maxima of **PP9**. Therefore, with blueshifted absorptions and comparable emission maxima, **PP13**–**14** demonstrate larger Stokes shifts. The molar absorptivities in dioxane were 25×10^3 and $33\times10^3\,M^{-1}cm^{-1}$, respectively. The quantum yields of these two dyes followed the same trends as the reference compounds **PP9** and **PP1** and fell nearly in the same range depending on the solvent used.

Finally, the methylenemalonitrile **PP15**–**16** with piperidine and morpholine groups were respectively synthesised to verify the potential synergic effect of the acceptor and donor on the photophysics (Table S4). The absorptions of **PP15--16** appeared in the visible range (440–475 nm, $34–36\times10^3\,M^{-1}cm^{-1}$), allowing a selective excitation with the blue diode (445 nm) or the argon ion laser line (488 nm). The fluorescence remained in the near-IR region (705–713 nm), yielding spectacular mega-Stokes shifts (DMSO and H_2O: 240–260 nm, toluene: 105 nm, Figure 7).

The $\mu_E-\mu_G$ values of **PP15**–**16** (14.4 and 14.9 D) were comparable to that of **PP4** (14.1 D). They were the highest among all of the studied dyes. The large dipole differences confirm the

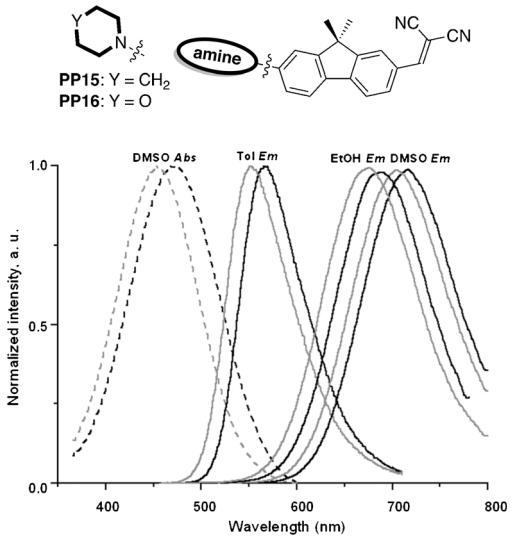

Figure 7. Absorbance (dashed lines) and emission (solid lines) spectra of the push–pull dyes **PP15** (black) and **PP16** (grey) in representative solvents.

strongest electron-withdrawing ability of the methylenemalonitrile, in agreement with the DFT calculations (Figure S7, Scheme S4). The quantum yields of **PP4**, **PP15** and **PP16** strongly correlate with the $E_T(30)$ scale, confirming the close relationship between the quantum yield and the sensitivity of the CT-type excited states to the polarity (Figure 8). The decrease in the emission intensity in polar solvents is typical for solvatochromic dyes with strong ICT character. It was advanced that the reduced energy gap between the excited and ground states in polar solvents favoured internal conversion and thus non-radiative energy release.[12] This linear trend can help to anticipate the emissive behaviour of the dyes with the strongest transition dipole moment in a medium of known polarity.

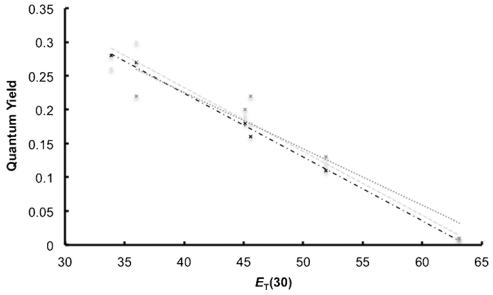

Figure 8. Dependence of the quantum yield for **PP4** (light grey), **PP15** (black) and **PP16** (dark grey) on the empirical polarity parameter $E_T(30)$. Linear trends were obtained with all the representative solvents, except chloroform (correlation factors R^2 are, respectively, 0.965, 0.996 and 0.87).

Hammett correlation

The correlations of the absorption and emission maxima to the σ_P Hammett substituent constants were assessed.[81] This approach could complement the challenging predictions of emission of fluorophores with CT in the excited state by TD-DFT.[82] Thus, four representative molecules were selected: **PP1** as a reference, **PP4** as the strongest acceptor, **PP12** as the weakest donor and **I-6** as a control.

As the D and A substituents in the fluorene derivatives present a mesomeric relationship like in *para*-disubstituted aromatic derivatives, the photophysics of the selected examples were depicted as a function of the σ_P values ($\sigma_P{}^A - \sigma_P{}^D$).[83] The absorption maxima of the whole set correlated strongly with the σ_P parameter, reflecting the difference between the electron-donating and -withdrawing properties of the substituents in the wide range of polarity (Figure 9).

In parallel, a linear trend between emission maxima and σ_P values was noticed exclusively with the dyes presenting large solvatofluorochromism (**PP1**, **PP12** and **PP4**, Figure 10). Indeed, as the emission occurs through a charge-transfer mechanism, this correlation is consistent with the observation that stabilisation of the excited states was highly sensitive to polarity. To verify these prediction models, the absorption and emission maxima of a reported fluorene dye (diethylamino D and formyl A) were calculated in three solvents (ethanol, acetonitrile and chloroform; Table S4).[21] The anticipated absorption maxima were in agreement with those recorded experimentally (Table S6 in the Supporting Information). The emission maxima were slightly redshifted (10–20 nm) compared with the experimental values. The error was within the acceptable margin. Hence, this model is an interesting tool to predict spectroscopic properties in the prerequisite design of advanced probes.

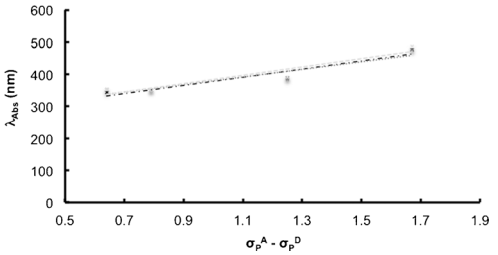

Figure 9. Dependence of the absorption maxima of **PP1**, **PP4**, **PP12** and **I-6** on the donor/acceptor Hammett σ_P value ($\sigma_P{}^A - \sigma_P{}^D$) in EtOH (black), acetonitrile (dark grey) and chloroform (light grey). Correlation factors R^2 are, respectively, 0.94, 0.89 and 0.91.

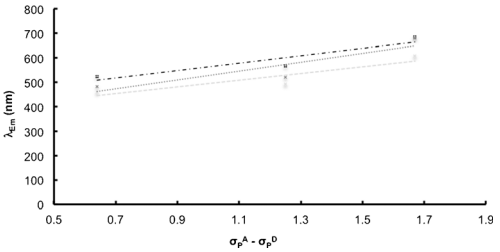

Figure 10. Dependence of the emission maxima of **PP1**, **PP4** and **PP12** on the donor/acceptor Hammett σ_P value ($\sigma_P{}^A - \sigma_P{}^D$) in EtOH (black), acetonitrile (dark grey) and chloroform (light grey). Correlation factors R^2 are, respectively, 0.88, 0.81 and 0.83.

Conclusion

To sum up, we rationally designed, synthesised and characterised a library of fluorescent push–pull dyes based on a 2,7-disubstituted fluorene scaffold. These emissive D–π–A derivatives were prepared by straightforward and gram-scalable synthetic pathways. Two different series were developed in which the acceptor and donor substituents were varied. The various electron-withdrawing groups were efficiently introduced on a common and easily accessible synthon by different methodologies, including, amongst others: Stille coupling, CuAAC and peptide coupling. The screening of the electron-donating groups was chemoselectively achieved by a versatile Buchwald–Hartwig amination on a fluorenyl carbaldehyde intermediate obtained by an optimised formylation reaction. Photophysical studies highlighted the most promising compounds in terms of brightness, mega-Stokes shift, excitation accessibility and versatility for subsequent conjugation. The propioloyl linker was introduced for conjugation and converted into the ketotriazolyl derivative whilst maintaining the desired optical properties. Such characteristics make the ynone a prospective anchoring point for biolabelling. By combining the attractive electron-donating (morpholine, piperidine) and electron-with-

drawing (methylenemalonitrile) groups, the synergic effect was tested. These studies led to new push–pull fluorenes with red-shifted absorption and emission. Owing to enhanced intramolecular charger transfer, the dyes were highly solvatofluorochromic over the entire polarity scale and even near-IR emissions were observed in protic solvents. DFT calculations confirmed these experimental observations. Correlation of a selected set of D–π–A emitters with Hammett σ_P values of the considered donor/acceptor pairs provides a complementary tool to anticipate the spectroscopic features desired for specific applications. The incorporation of these building blocks in DNA and membranes is the focus of our ongoing research and will be reported in due time.

Experimental Section

General information is provided in the Supporting Information.

Formylation procedure for 7-bromo-9,9-dimethylfluorene-2-carbaldehyde (8)

Cl_2CHOCH_3 (1.25 mL, 3.8 mmol, 1.5 equiv) was added dropwise to a stirred solution of **2** (2.50 g, 9.2 mmol, 1 equiv) and $ZrCl_4$ (3.20 g, 13.8 mmol, 1.5 equiv) [or $AlCl_3$] in CH_2Cl_2 (30 mL) at 0 °C under argon. The reaction mixture was stirred for 2 h at 0 °C then warmed to room temperature and poured into an ice-water bath (15 mL). The phases were separated and the aqueous phase was extracted twice with $CHCl_3$. The combined extracts were washed with water and saturated aq. $NaHCO_3$ solution, dried over $MgSO_4$ and concentrated in vacuo. The crude product was purified by flash chromatography on silica gel eluted with cyclohexane (CyHex)/CH_2Cl_2 (4:1, v/v) to afford the product **8** (2.10 g, 77%) as a bright-yellow solid. $C_{16}H_{13}BrO$ (301.18). $R_f = 0.16$ (CyHex/CH_2Cl_2 = 4:1); ^{1}H NMR (200 MHz, $CDCl_3$): $\delta = 10.06$ (s, 1H), 7.96 (d, $^4J = 1.0$ Hz, 1H), 7.88 (br d, $^3J = 8.0$ Hz, 1H), 7.84 (s, 1H), 7.68–7.61 (m, 2H), 7.52 (dd, $J = 8.0$, 2.0 Hz, 1H), 1.52 ppm (s, 6H); ^{13}C NMR (50 MHz, $CDCl_3$): $\delta = 192.1$, 157.0, 154.1, 144.6, 136.8, 135.9, 130.8, 130.7, 126.6, 123.2 (2C), 122.7, 120.5, 47.4, 26.9 ppm (2C); GC-MS (*m/z*): 302.1 [M^+].

1-(7-(Dimethylamino)-9,9-dimethyl-9*H*-fluoren-2-yl)prop-2-yn-1-one (PP2)

Ethynylmagnesium bromide (3.16 mL, 0.5 M in THF, 1.58 mmol, 1.4 equiv) was added dropwise to a solution of carbaldehyde **PP1** (300 mg, 1.13 mmol, 1 equiv) in THF (2.5 mL) at 0 °C. The mixture was stirred at the same temperature until the completion of the reaction (2 h). Then, a saturated solution of aq. NH_4Cl (3 mL) was added and the aqueous phase was extracted with EtOAc (3× 5 mL). The combined extracts were dried (magnesium sulfate), filtered and evaporated to yield the corresponding propargyl alcohol. The crude propargyl alcohol was used in the next step without further purification. A solution of the residue in 1,2-dichloroethane (3 mL, DCE) was added dropwise to a stirred suspension of MnO_2 (0.5 g, 15 equiv) in DCE (8 mL). The mixture was stirred for 1 h at 0 °C, filtered through a pad of Celite®, dried over $MgSO_4$ and concentrated in vacuo to yield the pure ketone **PP2** (320 mg, 98%, two steps). $R_f = 0.55$ (PE/EtOAc = 6:1); ^{1}H NMR (200 MHz, $CDCl_3$): $\delta = 8.18$–8.13 (m, 2H), 7.68–7.61 (m, 2H), 6.76–6.73 (br s, 2H), 3.41 (s, 1H), 3.08 (s, 6H), 1.50 ppm (s, 6H); ^{13}C NMR (50 MHz, $CDCl_3$): $\delta =$ 177.0, 157.4, 153.1, 151.7, 147.0, 133.4, 130.9, 126.1, 123.0, 122.4, 118.2, 111.7, 105.9, 81.0, 80.1, 46.8, 40.7 (2C), 27.3 ppm (2C); HRMS (ESI$^+$): *m/z* calcd for $C_{20}H_{20}ON$: 290.1539 [$M+H$]$^+$; found: 290.1539.

(7-(Dimethylamino)-9,9-dimethyl-9*H*-fluoren-2-yl)(1-hexyl-1*H*-1,2,3-triazol-4-yl)methanone (PP3)

A solution of **PP2** (60 mg, 0.21 mmol, 1 equiv) in DCE (1 mL) was added dropwise to a stirred solution of *n*-hexyl azide (30 mg, 0.23 mmol, 1.1 equiv) in DCE (1 mL) at 0 °C under argon. Then, *N*,*N*-diisopropylethylamine (DIEA) (0.18 mL, 1.4 mmol, 5 equiv), CuI (78 mg, 0.41 mmol, 2 equiv) and AcOH (12 μL, 0.1 mmol, 1 equiv) were sequentially added. The reaction mixture was stirred at room temperature for 3 h, filtered over a pad of Decalite® and washed with CH_2Cl_2. The solvents were evaporated and the resulting crude product was purified by flash chromatography on silica gel eluted with CyHex/EtOAc (94:6, v/v) to provide **PP3** (30 mg, 70%) as a yellow powder. $R_f = 0.15$ (CyHex/EtOAc = 94:6); ^{1}H NMR (200 MHz, $CDCl_3$): $\delta = 8.55$ (dd, $J = 8.0$, 1.5 Hz, 1H, H3), 8.52 (d, $^4J = 1.5$ Hz, 1H, H1), 8.25 (s, 1H, $H_{triazole}$), 7.67 (d, $^3J = 8.0$ Hz, 2H, H4,5), 6.77 (s, 1H, H8), 6.75 (d, $^3J = 8.0$ Hz, 1H, H6), 4.45 (t, $^3J = 7.0$ Hz, 2H, H1′), 3.07 (s, 6H, $N(CH_3)_2$), 1.98 (m, 2H, H2′), 1.53 (s, 6H, $2CH_3$ 9,9), 1.36–1.26 (m, 6H, H3′,4′,5′), 0.90 ppm (t, $^3J = 7.0$ Hz, 3H, H6′); ^{13}C NMR (50 MHz, $CDCl_3$): $\delta = 185.3$ (C=O), 157.2 (C_a), 152.9 (C_b), 151.5 (C7), 148.9 (C=CH), 145.6 (C_d), 133.5 (C2), 131.3 (C3), 128.1 (C=CH), 126.9 (C_c), 124.5 (C1), 122.2 (C5), 118.1 (C4), 111.7 (C6), 106.2 (C8), 50.7 (C1′), 47.0 (C9), 40.9 (2C, $N(CH_3)_2$), 31.2 (C4′), 30.3 (C2′), 27.5 (2C, $2CH_3$), 26.2 (C3′), 22.5 (C5′), 14.1 ppm (C6′); HRMS (ESI$^+$): *m/z* calcd for $C_{26}H_{33}N_4O$: 417.2649 [$M+H$]$^+$; found: 417.2649.

General procedure (GP-A) for malonitriles (PP4 and PP15–16)

Malononitrile (2 equiv) and basic aluminium oxide (4 equiv) were added to a 0.2 M solution of 7-alkylamino-9,9-dimethyl-9*H*-fluorene-2-carbaldehyde (1 equiv) in toluene. The mixture was stirred overnight at 70 °C. After cooling to room temperature, the reaction mixture was filtered and the solvents were removed in vacuo. The crude product was purified by silica gel column chromatography to provide the desired product as a bright-red solid (for details, see the Supporting Information).

General procedure of Buchwald–Hartwig amination (GP-B) for PP7–14

A solution of *t*BuONa (1.2 equiv), $Pd(OAc)_2$ (5 mol%) and BINAP (10 mol%) in toluene was stirred for 15 min under argon. Subsequently, **8** (1 equiv) and the amine (liquid or dissolved in toluene, 1.2 equiv) were added. The final concentration of compound **8** in toluene was 0.1 M. After further stirring for 15 min, the reaction mixture was irradiated in the microwave oven at 300 W/180 °C for 20 to 30 min (or classically heated at 100 °C in an oil bath overnight in the case of products that were experimentally demonstrated to have a lower stability as observed by relatively lower yields). The reaction was monitored by TLC/GC until complete conversion. Then, the resulting mixture was cooled to room temperature, diluted with CH_2Cl_2 and filtered over a pad of Celite®. The solvents were removed under reduced pressure, and the residue was purified by silica gel column chromatography to give the desired product (for details, see the Supporting Information).

Acknowledgements

We thank the ANR (ANR-12-BS08-0003-02), PACA région (DNAfix-2014-02862 and 2014-07199) and the FRM (DCM20111223038) for financial support and the French Government for the grant to J.S. We are grateful to J.-F. Gal and J. Wytko for their fruitful comments and critical reading of the manuscript.

Keywords: Buchwald–Hartwig amination · charge transfer · fluorescent probes · push–pull fluorenes · structure–photophysics relationship

[1] A. S. Klymchenko, Y. Mély, Fluorescent Environment-Sensitive Dyes as Reporters of Biomolecular Interactions in *Progress in Molecular Biology and Translational Science, Vol. 113* (Ed.: M. C. Morris), Academic Press, Burlington, **2013**, pp. 35 – 58.
[2] H. Meier, *Angew. Chem. Int. Ed.* **2005**, *44*, 2482; *Angew. Chem.* **2005**, *117*, 2536.
[3] M. Kivala, F. Diederich, *Pure Appl. Chem.* **2008**, *80*, 411.
[4] S.-I. Kato, F. Diederich, *Chem. Commun.* **2010**, *46*, 1994.
[5] F. Bureš, *RSC Adv.* **2014**, *4*, 58826.
[6] C. Reichardt, *Chem. Rev.* **1994**, *94*, 2319.
[7] A. Marini, A. Muñoz-Losa, A. Biancardi, B. Mennucci, *J. Phys. Chem. B* **2010**, *114*, 17128.
[8] Z. Diwu, Y. Lu, C. Zhang, D. H. Klaubert, R. P. Haugland, *Photochem. Photobiol.* **1997**, *66*, 424.
[9] R. J. Brea, M. E. Vázquez, M. Mosquera, L. Castedo, J. R. Granja, *J. Am. Chem. Soc.* **2007**, *129*, 1653.
[10] Z. Lu, S. J. Lord, H. Wang, W. E. Moerner, R. J. Twieg, *J. Org. Chem.* **2006**, *71*, 9651.
[11] K. Tainaka, K. Tanaka, S. Ikeda, K.-I. Nishiza, T. Unzai, Y. Fujiwara, I. Saito, A. Okamoto, *J. Am. Chem. Soc.* **2007**, *129*, 4776.
[12] Y. Niko, S. Kawauchi, G.-I. Konishi, *Chem. Eur. J.* **2013**, *19*, 9760.
[13] E. Benedetti, L. S. Kocsis, K. M. Brummond, *J. Am. Chem. Soc.* **2012**, *134*, 12418.
[14] I. V. Kurdyukova, A. A. Ishchenko, *Russ. Chem. Rev.* **2012**, *81*, 258.
[15] a) J. R. Lakowicz, *Principles of Fluorescence Spectroscopy*, 3rd ed., Springer, New York, **2006**, pp. 954; b) B. Valeur, M. N. Berberan-Santos, *Molecular Fluorescence: Principles and Applications*, 2nd ed., Wiley-VCH, Weinheim, **2012**, pp. 592.
[16] A. V. Kulinich, N. A. Derevyanko, A. A. Ishchenko, S. L. Bondarev, V. N. Knyukshto, *J. Photochem. Photobiol. A* **2008**, *200*, 106.
[17] I. Baraldi, F. Momicchioli, G. Ponterini, A. S. Tatikolov, D. Vanossi, *Phys. Chem. Chem. Phys.* **2003**, *5*, 979.
[18] J. Zhao, W. Wu, J. Sun, S. Guo, *Chem. Soc. Rev.* **2013**, *42*, 5323.
[19] F. E. Hernández, K. D. Belfield, I. Cohanoschi, *Chem. Phys. Lett.* **2004**, *391*, 22.
[20] I. Cohanoschi, K. D. Belfield, F. E. Hernández, *Chem. Phys. Lett.* **2005**, *406*, 462.
[21] a) O. A. Kucherak, P. Didier, Y. Mély, A. S. Klymchenko, *J. Phys. Chem. Lett.* **2010**, *1*, 616; b) S. Sasaki, Y. Niko, A. S. Klymchenko, G.-I. Konishi, *Tetrahedron* **2014**, *70*, 7551.
[22] K. D. Belfield, M. V. Bondar, O. V. Przhonska, K. J. Schafer, *J. Photochem. Photobiol. A* **2004**, *162*, 569.
[23] C. Díaz, A. Frazer, A. Morales, K. D. Belfield, S. Ray, F. E. Hernández, *J. Phys. Chem. A* **2012**, *116*, 2453.
[24] K. D. Belfield, M. V. Bondar, O. V. Przhonska, K. J. Schafer, *Photochem. Photobiol. Sci.* **2004**, *3*, 138.
[25] K. J. Schafer-Hales, K. D. Belfield, S. Yao, P. K. Frederiksen, J. M. Hales, P. E. Kolattukudy, *J. Biomed. Opt.* **2005**, *10*, 051402.
[26] S. Yao, K. D. Belfield, *Eur. J. Org. Chem.* **2012**, *2012*, 3199.
[27] K. Rathore, C. S. Lim, Y. Lee, B. R. Cho, *Org. Biomol. Chem.* **2014**, *12*, 3406.
[28] B. A. Reinhardt, L. L. Brott, S. J. Clarson, A. G. Dillard, J. C. Bhatt, R. Kannan, L. Yuan, G. S. He, P. N. Prasad, *Chem. Mater.* **1998**, *10*, 1863.
[29] H. Zhang, J. Fan, H. Dong, S. Zhang, W. Xu, J. Wang, P. Gao, X. Peng, *J. Mater. Chem. B* **2013**, *1*, 5450.
[30] X. Yue, C. O. Yanez, S. Yao, K. D. Belfield, *J. Am. Chem. Soc.* **2013**, *135*, 2112.
[31] M. A. Oar, J. M. Serin, W. R. Dichtel, J. M. J. Fréchet, T. Y. Ohulchanskyy, P. N. Prasad, *Chem. Mater.* **2005**, *17*, 2267.
[32] F. E. Hernández, K. D. Belfield, I. Cohanoschi, M. Balu, K. Schafer, *Appl. Opt.* **2004**, *43*, 5394.
[33] K. Rathore, C. S. Lim, Y. Lee, H. J. Park, B. R. Cho, *Asian J. Org. Chem.* **2014**, *3*, 1070.
[34] A. Frazer, A. R. Morales, A. W. Woodward, P. Tongwa, T. Timofeeva, K. D. Belfield, *J. Fluoresc.* **2013**, *23*, 239.
[35] X. Dong, J. H. Han, C. H. Heo, H. M. Kim, Z. Liu, B. R. Cho, *Anal. Chem.* **2012**, *84*, 8110.
[36] S. Wang, G. C. Bazan, *Chem. Commun.* **2004**, 2508.
[37] I. Fischer, A. P. H. J. Schenning, Nanoparticles Based on π-Conjugated Polymers and Oligomers for Optoelectronic Imaging, and Sensing Applications: The Illustrative Example of Fluorene-Based Polymers and Oligomers, in *Organic Electronics: Emerging Concepts and Technologies*, (Eds.: F. Cicoira, C. Santato), Wiley-VCH, Weinheim, **2013**, pp. 1 – 25.
[38] M. J. Kim, Y. Seo, G. T. Hwang, *RSC Adv.* **2014**, *4*, 12012.
[39] J. Guo, T. Wang, R. Yang, *Mol. BioSyst.* **2012**, *8*, 2347.
[40] D. Wenger, V. L. Malinovskii, R. Häner, *Chem. Commun.* **2011**, *47*, 3168.
[41] E. Ergen, M. Weber, J. Jacob, A. Herrmann, K. Müllen, *Chem. Eur. J.* **2006**, *12*, 3707.
[42] G. C. Bazan, S. Wang, in *Organic Semiconductors in Sensor Applications*, Springer, Berlin, Heidelberg, **2008**, pp. 1 – 37.
[43] A. R. Morales, C. O. Yanez, K. J. Schafer-Hales, A. I. Marcus, K. D. Belfield, *Bioconjugate Chem.* **2009**, *20*, 1992.
[44] V. Singh, S. Wang, E. T. Kool, *J. Am. Chem. Soc.* **2013**, *135*, 6184.
[45] X. Yue, Z. Armijo, K. King, M. V. Bondar, A. R. Morales, A. Frazer, I. A. Mikhailov, O. V. Przhonska, K. D. Belfield, *ACS Appl. Mater. Interfaces* **2015**, *7*, 2833.
[46] Y. Wang, Y. Gao, L. Chen, Y. Fu, D. Zhu, Q. He, H. Cao, J. Cheng, R. Zhang, S. Zheng, *RSC Adv.* **2014**, *4*, 4853.
[47] C. Mallet, M. Le Borgne, M. Starck, W. G. Skene, *Polym. Chem.* **2013**, *4*, 250.
[48] A. C. Grimsdale, K. Müllen, in *Emissive Materials Nanomaterials*, Springer, Berlin, Heidelberg, **2006**, pp. 1 – 82.
[49] J. U. Wallace, S. H. Chen, in *Polyfluorenes* (Eds.: U. Scherf, D. Neher), Springer, Berlin, Heidelberg, **2008**, pp. 145 – 186.
[50] R. S. Kularatne, H. D. Magurudeniya, P. Sista, M. C. Biewer, M. C. Stefan, *J. Polym. Sci. Part A* **2013**, *51*, 743.
[51] M. Romain, S. Thiery, A. Shirinskaya, C. Declairieux, D. Tondelier, B. Geffroy, O. Jeannin, J. Rault-Berthelot, R. Métivier, C. Poriel, *Angew. Chem. Int. Ed.* **2014**, *53*, 11333; *Angew. Chem.* **2014**, *126*, 11515.
[52] K. Ogawa, *Appl. Sci.* **2014**, *4*, 1.
[53] X.-D. Zhuang, Y. Chen, B.-X. Li, D.-G. Ma, B. Zhang, Y. Li, *Chem. Mater.* **2010**, *22*, 4455.
[54] a) D. Dziuba, I. A. Karpenko, N. P. F. Barthes, B. Y. Michel, A. S. Klymchenko, R. Benhida, A. P. Demchenko, Y. Mély, A. Burger, *Chem. Eur. J.* **2014**, *20*, 1998; b) N. P. F. Barthes, I. A. Karpenko, D. Dziuba, M. Spadafora, J. Auffret, A. P. Demchenko, Y. Mely, R. Benhida, B. Y. Michel, A. Burger, *RSC Adv.* **2015**, *5*, 33536; c) N. P. F. Barthes, K. Gavvala, D. Dziuba, D. Bonhomme, I. A. Karpenko, A. S. Dabert-Gay, D. Debayle, A. P. Demchenko, R. Benhida, B. Y. Michel, Y. Mély, A. Burger, *J. Mater. Chem. C* **2016**, *4*, 3010.
[55] a) G. Mignani, F. Leising, R. Meyrueix, H. Samson, *Tetrahedron Lett.* **1990**, *31*, 4743; b) A. R. Morales, A. Frazer, A. W. Woodward, H.-Y. Ahn-White, A. Fonari, P. Tongwa, T. Timofeeva, K. D. Belfield, *J. Org. Chem.* **2013**, *78*, 1014.
[56] B. Strehmel, A. Sarker, H. Detert, *ChemPhysChem* **2003**, *4*, 249.
[57] a) T. Peng, D. Yang, *Org. Lett.* **2010**, *12*, 4932; b) L. Wu, K. Burgess, *J. Org. Chem.* **2008**, *73*, 8711.
[58] K. Nomura, N. Yamamoto, R. Ito, M. Fujiki, Y. Geerts, *Macromolecules* **2008**, *41*, 4245.
[59] Y. Wang, J. Zhou, X. Wang, X. Zheng, Z. Lu, W. Zhang, Y. Chen, Y. Huang, X. Pu, J. Yu, *Dyes Pigm.* **2014**, *100*, 87.
[60] C. L. Chiang, M. F. Wu, D. C. Dai, Y. S. Wen, J. K. Wang, C. T. Chen, *Adv. Funct. Mater.* **2005**, *15*, 231.
[61] P. J. Homnick, P. M. Lahti, *Phys. Chem. Chem. Phys.* **2012**, *14*, 11961.

[62] J.-Z. Cheng, C.-C. Lin, P.-T. Chou, A. Chaskar, K.-T. Wong, *Tetrahedron* **2011**, *67*, 734.
[63] L. Y. Chiang, P. A. Padmawar, T. Canteenwala, L.-S. Tan, G. S. He, R. Kannan, R. Vaia, T.-C. Lin, Q. Zheng, P. N. Prasad, *Chem. Commun.* **2002**, 1854.
[64] W. H. Nguyen, C. D. Bailie, J. Burschka, T. Moehl, M. Grätzel, M. D. McGehee, A. Sellinger, *Chem. Mater.* **2013**, *25*, 1519.
[65] G. Saroja, Z. Pingzhu, N. P. Ernsting, J. Liebscher, *J. Org. Chem.* **2004**, *69*, 987.
[66] M. R. Schrimpf, K. B. Sippy, C. A. Briggs, D. J. Anderson, T. Li, J. Ji, J. M. Frost, C. S. Surowy, W. H. Bunnelle, M. Gopalakrishnan, M. D. Meyer, *Bioorg. Med. Chem. Lett.* **2012**, *22*, 1633.
[67] J. K. Sørensen, J. Fock, A. H. Pedersen, A. B. Petersen, K. Jennum, K. Bechgaard, K. Kilså, V. Geskin, J. Cornil, T. Bjørnholm, M. B. Nielsen, *J. Org. Chem.* **2011**, *76*, 245.
[68] J. F. Hartwig, S. Richards, D. Barañano, F. Paul, *J. Am. Chem. Soc.* **1996**, *118*, 3626.
[69] W. H. Melhuish, *J. Phys. Chem.* **1961**, *65*, 229.
[70] S. M. Ormson, R. G. Brown, F. Vollmer, W. Rettig, *J. Photochem. Photobiol. A* **1994**, *81*, 65.
[71] M. Shimizu, K. Mochida, M. Katoh, T. Hiyama, *J. Phys. Chem. C* **2010**, *114*, 10004; b) A. Baheti, P. Singh, K. R. J. Thomas, *Dyes Pigm.* **2011**, *88*, 195.
[72] a) E. Z. Lippert, *Z. Naturforsch.* **1955**, *10*, 541; b) N. Mataga, Y. Kaifu, M. Koizumi, *Bull. Chem. Soc. Jpn.* **1956**, *29*, 465.
[73] a) J. B. Grimm, B. P. English, J. Chen, J. P. Slaughter, Z. Zhang, A. Revyakin, R. Patel, J. J. Macklin, D. Normanno, R. H. Singer, T. Lionnet, L. D. Lavis, *Nat. Methods* **2015**, *12*, 244.
[74] A. T. Krueger, B. Imperiali, *ChemBioChem* **2013**, *14*, 788.
[75] Y. Deng, W. Yuan, Z. Jia, G. Liu, *J. Phys. Chem. B* **2014**, *118*, 14536.
[76] R. A. Moore, J. Lee, G. W. Robinson, *J. Phys. Chem.* **1985**, *89*, 3648.
[77] a) R. R. Gupta, M. Kumar, V. Gupta, in *Heterocyclic Chemistry*, Springer, Berlin, Heidelberg, **1998**, pp. 275 – 355; b) O. C. Dermer, G. E. Ham, in *Ethyleneimine and Other Aziridines. Chemistry and Applications*, Academic Press, New York, **1969**, pp. 592; c) D. Tanner, C. Birgersson, *Tetrahedron Lett.* **1991**, *32*, 2533; d) A. de Meijere, *Angew. Chem. Int. Ed. Engl.* **1979**, *18*, 809: Angew. Chem. **1979**, 91, 867 – 884.
[78] T. Ohwada, H. Hirao, A. Ogawa, *J. Org. Chem.* **2004**, *69*, 7486.
[79] a) F. Liu, W. Du, Q. Liang, Y. Wang, J. Zhang, J. Zhao, S. Zhu, *Tetrahedron* **2010**, *66*, 5467; b) B. Lu, J. Zhang, J. Li, J. Yao, M. Wang, Y. Zou, S. Zhu, *Tetrahedron* **2012**, *68*, 8924.
[80] J.-C. Kuhlmann, P. de Bruyn, R. K. M. Bouwer, A. Meetsma, P. W. M. Blom, J. C. Hummelen, *Chem. Commun.* **2010**, *46*, 7232.
[81] Selected examples of correlations involving the Hammett substituent constants and spectroscopic properties: a) S. K. Christa, J. J. M. Thomas, *Eur. J. Org. Chem.* **2003**, 3534; b) R. Pohl, V. A. Montes, J. Shinar, P. Anzenbacher Jr, *J. Org. Chem.* **2004**, *69*, 1723; c) Y. Yamaguchi, T. Tanaka, S. Kobayashi, T. Wakamiya, Y. Matsubara, Z. Yoshida, *J. Am. Chem. Soc.* **2005**, *127*, 9332; d) C.-C. Chao, M. Leung, *J. Org. Chem.* **2005**, *70*, 4323; e) G. R. Potter, S. T. Hughes, *J. Org. Chem.* **2008**, *73*, 2995; f) D. F. Perepichka, I. F. Perepichka, *Chem. Eur. J.* **2008**, *14*, 2757; g) C.-H. Zhao, E. Sakuda, A. Wakamiya, S. Yamaguchi, *Chem. Eur. J.* **2009**, *15*, 10603; h) F. L. Ciscato, H. F. Bartoloni, D. Weiss, R. Beckert, J. W. Baader, *J. Org. Chem.* **2010**, *75*, 6574; i) E. Yamaguchi, F. Shibahara, T. Murai, *J. Org. Chem.* **2011**, *76*, 6146; j) M. Kovaliov, M. Weitman, D. T. Major, B. Fischer, *J. Org. Chem.* **2014**, *79*, 7051; k) P. A. Hopkins, R. W. Sinkeldam, Y. Tor, *Org. Lett.* **2014**, *16*, 5290.
[82] D. W. Silverstein, N. Govind, H. J. J. van Dam, L. Jensen, *J. Chem. Theory Comput.* **2013**, *9*, 5490.
[83] C. Hansch, A. Leo, R. W. Taft, *Chem. Rev.* **1991**, *91*, 165.

Received: February 7, 2016
Published online on ■■ ■■, 0000

FULL PAPER

Fluorescent Probes

*J. Shaya, F. Fontaine-Vive, B. Y. Michel, A. Burger**

■■ – ■■

Rational Design of Push–Pull Fluorene Dyes: Synthesis and Structure–Photophysics Relationship

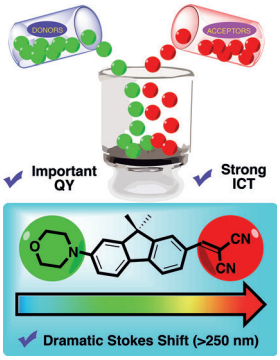

Building a fluorescent LEGO box: Based on a fluorene scaffold, the design, robust synthesis, and characterization of a library of dyes is reported. The dyes have varying push–pull strengths, important solvatofluorochromism properties, and suitable anchoring groups for conjugation. DFT calculations support an enhanced intramolecular charge transfer from which their near-IR emission originates. The Hammett prediction model provides a tool to anticipate the photophysical properties.